Bionatura

ISSN 1390-9355
Vol.11. No 3. 2026

Research Article

Interaction Mechanisms of Bioactive Compounds with α-Synuclein: A Docking and Molecular Dynamics Study

Yasmir Quiroz[1,], Ariana Delgado[2], Marylu Mora[3], Alejandro Vivas[4], Aníbal Méndez[5], Bravo Yanauri[6], Ysaías Alvarado[7], Lenin González-Paz[8]*

[1]*Instituto Venezolano de Investigaciones Científicas. Maracaibo. Venezuela. https://orcid.org/0009-0005-4300-697*

[2]*Instituto Venezolano de Investigaciones Científicas. Maracaibo. Venezuela. https://orcid.org/0000-0003-2426-779X*

[3]*Instituto Venezolano de Investigaciones Científicas. Maracaibo. Venezuela. https://orcid.org/0000-0002-7826-2815*

[4]*Instituto Venezolano de Investigaciones Científicas. Maracaibo. Venezuela. https://orcid.org/0000-3 0001-6750-8712*

[5]*Instituto Venezolano de Investigaciones Científicas. Maracaibo. Venezuela. https://orcid.org/0000-0003-2162-400X*

[6]*Instituto Venezolano de Investigaciones Científicas. Maracaibo. Venezuela. https://orcid.org/0009-0000-3147-7539*

[7]*Instituto Venezolano de Investigaciones Científicas. Maracaibo. Venezuela. https://orcid.org/0000-0002-2709-409X*

[8]*Instituto Venezolano de Investigaciones Científicas. Maracaibo. Venezuela. https://orcid.org/0000-0003-0023-7342*

Correspondence: yasmir.quiroz@gmail.com.

Available from: https://revistabionatura.org/files-web/. (Doi10.70373/RB/2026.11.03.2)

Abstract

Alpha-synuclein (αSN) is an intrinsically disordered protein whose aggregation is closely linked to Parkinson's disease. Its inherent structural plasticity, however, hinders the identification of ligand-binding regions capable of modulating pro-aggregating conformations. In this study, we conducted a comparative computational analysis to examine the interaction patterns of 38 bioactive compounds from six chemical classes with micelle-bound αSN. Blind docking revealed scaffold-dependent binding patterns across the protein sequence. Specifically, polyphenols and flavonoids interacted predominantly with the C-terminal regulatory region, whereas terpenes and polyunsaturated fatty acids favored the N-terminal membrane-binding segment and the region adjacent to the non-amyloid component (NAC). Representative complexes were further evaluated through explicit-solvent molecular dynamics simulations. Notably, ligand-driven modulation of protein flexibility proved compound-specific, with several molecules inducing localized reductions in fluctuations within key aggregation-prone regions. This work establishes a comparative structural framework for the interaction of diverse bioactive molecules with αSN, providing distinct interaction signatures to guide the rational design of future therapeutic modulators.

Keywords

Parkinson's disease; Protein aggregation; Bioactive compounds; Intrinsically disordered proteins (IDPs).

Introduction

α-Synuclein (αSN) is a 140–amino acid presynaptic protein enriched in the central nervous system, where it regulates synaptic vesicle trafficking, neurotransmitter release, and synaptic plasticity.[1,2] Under pathological conditions, αSN misfolds and self-associates into toxic oligomers and amyloid fibrils that accumulate in Lewy bodies, the neuropathological hallmark of Parkinson's disease (PD) and related synucleinopathies.[2,3] Mutations or overexpression of the αSN gene accelerate aggregation and are causally linked to familial PD, supporting αSN dysfunction as an early molecular event in both inherited and sporadic disease.[4–6]

Beyond dopaminergic neuron vulnerability, αSN pathology contributes to mitochondrial dysfunction, oxidative stress, impaired proteostasis, lysosomal deficits, and neuroinflammation, exacerbating neuronal degeneration.[7,8] Uptake of misfolded αSN by glial cells can further amplify inflammatory responses, promoting a feed-forward cycle of neuronal injury and disease progression.[9,10] Structurally, αSN belongs to the intrinsically disordered proteins (IDPs) and exists as a highly dynamic conformational ensemble lacking a dominant folded state; while this intrinsic disorder enables functional plasticity, it also underlies the protein's propensity for pathological misfolding and aggregation.[11]

Upon interaction with lipid membranes or membrane-mimetic environments, αSN undergoes partial folding into α-helical conformations that precede pathological aggregation. The NMR-resolved micelle-bound structure (PDB ID: 1XQ8) reveals two antiparallel helices spanning the N-terminal and Non-amyloid Component (NAC) regions connected by a flexible linker, with the C-terminal domain remaining largely disordered.[12] Although micelle-bound structures do not fully reproduce physiological membrane conditions, this semi-folded state is widely used as a structural proxy for modeling early aggregation-prone conformations preceding pathogenic β-sheet–rich assemblies.

From a molecular recognition perspective, αSN is a challenging therapeutic target due to its intrinsic disorder, transient binding surfaces, and conformational heterogeneity. Conventional structure-based strategies developed for globular proteins are often insufficient for IDPs, where ligand binding occurs through dynamic, weakly populated interfaces rather than well-defined pockets, requiring ensemble-based and dynamic descriptors to evaluate ligand-induced modulation of aggregation-relevant states. In this context, computational approaches are valuable tools for probing αSN–ligand interactions at atomic resolution: molecular docking enables identification of preferential interaction regions,

ISSN 1390-9355
Vol.11. No 3. 2026

whereas molecular dynamics (MD) simulations provide insight into temporal stability, conformational heterogeneity, and residue-level modulation.[13,14]

Accumulating evidence indicates that natural bioactive compounds can modulate protein misfolding and aggregation pathways, including those involving αSN. Epidemiological studies associate dietary patterns rich in polyphenols, terpenes, and polyunsaturated fatty acids—particularly the Mediterranean diet—with reduced risk or delayed onset of PD.[15–17] Experimental models further show that polyphenols, carotenoids, and omega-3 fatty acids can interfere with amyloidogenic processes and exert antioxidant, anti-inflammatory, and autophagy-promoting effects relevant to PD pathophysiology.[18–21] However, the structural and dynamic basis by which chemically diverse natural compounds interact with αSN and influence its aggregation landscape remains insufficiently characterized.

Here, we present a systematic in silico evaluation of natural and pharmacologically relevant compounds to explore structure–interaction relationships and identify molecular scaffolds capable of engaging aggregation-relevant regions of αSN. By integrating molecular docking with MD simulations, we characterize scaffold-dependent interaction fingerprints and evaluate whether selected compounds modulate αSN conformational dynamics by stabilizing non-aggregating ensembles or by interfering with early nucleation and oligomerization interfaces. These analyses provide a mechanistically grounded computational framework for prioritizing bioactive compounds for subsequent experimental validation

Materials and methods

Selection of Protein and Compounds of Interest

The three-dimensional structure of human αSN was obtained from the Protein Data Bank (PDB ID: 1XQ8), corresponding to an NMR-resolved micelle-bound conformation that represents an early, aggregation-relevant structural state of the protein.[12] This conformation captures the partially ordered α-helical arrangement adopted by αSN upon interaction with membrane-mimetic environments and has been widely used as a structural proxy for studying early misfolding events, ligand binding, and aggregation-prone conformations in intrinsically disordered proteins.

Prior to molecular docking, the protein structure was preprocessed by removing crystallographic water molecules, repairing incomplete residues, adding hydrogen atoms, and optimizing side-chain geometry. Structural refinement was performed using the GalaxyRefine server (https://galaxy.seoklab.org/index.html),[22] with default parameters for mild stereochemical relaxation, including side-chain optimization and removal of local steric clashes. Although GalaxyRefine was

originally developed for globular proteins, it was applied here exclusively for local refinement without imposing secondary structure restraints, in order to preserve the intrinsically disordered character of αSN. Structural quality and stereochemical consistency were evaluated using MolProbity (http://molprobity.biochem.duke.edu/),[23] confirming acceptable backbone geometry, side-chain conformations, and the absence of major steric conflicts.

A total of 38 natural and pharmacologically relevant compounds were selected based on published evidence of neuroprotective, anti-inflammatory, antioxidant, or anti-amyloidogenic activity. The selected molecules encompassed six chemical classes with documented relevance to neurodegenerative disorders: essential fatty acids, terpenes, triterpenic acids, phenols, flavonoids/isoflavonoids, and alkaloids/drug. Chemical structures were retrieved from the PubChem database[24] in three-dimensional formats suitable for molecular docking simulations.

List of compounds, PubChem CIDs, and abbreviations used in this study: Eicosapentaenoic acid (EPA) CID: 5282847; Docosahexaenoic acid (DHA) CID: 445580 ; Icosapent ethyl (IPE) CID:446284; Linoleic acid (LA) CID: 5280450; Linolenic acid (ALA) CID: 5280934; Carvacrol (CAR) CID: 10364; Thymol (Thm) CID: 6989; α-Terpinene (α-Tpn) CID: 7462; γ-Terpinene (γ-Tpn) CID: 7461; Myrcene (Myr) CID: 31253; ρ-Cymene (ρ-Cym) CID: 7463; α-Humulene (α-Hum) CID: 5281520; Limonene (Lim) CID: 440917; Uvaol (Uva) CID: 92802; Ursolic Acid (UA) CID: 64945; Maslinic acid (Mas) CID: 73659; Erythrodiol (Ery) CID: 101761; Oleanolic acid (OA) CID: 10494; Eugenol (Eug) CID: 3314; Rosmarinic acid (RA) CID: 5281792; Tyrosol (Tyr) CID: 10393; Hydroxytyrosol (HTyr) CID: 82755; Caffeic acid (CA) CID: 689043; Verbascoside (Verb) CID: 5281800; Curcumin (Cur) CID: 969516; Oleocanthal (Ole) CID: 11652416; Resveratrol (Resv) CID: 445154; Scutellarein (Scu) CID: 5281697; Morin (Mor) CID: 5281670; Genistein (Gen) CID: 5280961; Formononetin (For) CID: 5280378; Epicatechin (EC) CID: 72276; Astragalin (Ast) CID: 5282102; Quercetin (Quer) CID: 5280343; Pregabalin (Preg) CID: 5486971; Gabapentin (Gab) CID: 3446; Melatonin (Mel) CID: 896; Caffeine (Caf) CID: 2519.

Ligand structures were prepared and energy-minimized using Avogadro (https://avogadro.cc/) with default force field parameters to obtain low-energy conformers.[25] Structural inspection, visualization, and file preparation were performed using Molegro Molecular Viewer and BIOVIA Discovery Studio Visualizer to verify chemical integrity, protonation states, and conformational suitability for docking.[26-29]

Molecular Docking

Protein–ligand docking was carried out using CB-Dock2 (http://clab.labshare.cn/cb-dock/), an automated blind docking platform that integrates cavity detection, grid box generation, and binding

ISSN 1390-9355
Vol.11. No 3. 2026

pose prediction based on the AutoDock Vina scoring function.[30,31] Docking calculations were performed using the server's default parameters, which are optimized for general protein–ligand screening and ensure consistency across ligands. For each compound, CB-Dock2 automatically identified putative binding cavities and generated ranked docking poses.

To reduce bias associated with reliance on a single scoring function and to improve robustness of relative ligand ranking, the top-ranked docking poses were further evaluated using multiple scoring functions implemented in Molegro Molecular Viewer, including MolDock Score, Rerank Score, and PLANTS Score. These scoring metrics were used exclusively for comparative and qualitative assessment of ligand–protein interaction propensities, rather than as absolute estimates of binding free energy. Given the conformational heterogeneity of intrinsically disordered proteins, docking was employed as an exploratory tool to identify preferential interaction regions and relative trends across a chemically diverse ligand set.

Molecular Dynamics Simulations

Following molecular docking and multi-score ranking, MD simulations were performed on a subset of αSN–ligand complexes selected according to a class-based strategy. For each chemical class evaluated, the ligand exhibiting the highest average docking score across all scoring functions was selected as a representative compound (Table S1). This strategy was designed to capture chemically driven interaction mechanisms while avoiding redundancy among structurally related ligands and enabling comparative analysis of ligand-induced effects across distinct bioactive scaffolds. An unbound αSN system was simulated in parallel as a reference.

All MD simulations were carried out using the OPMD module of the MyPresto 5 molecular simulation package[32,33] employing the AMBER ff14SB force field for the protein and the TIP3P water model for explicit solvation. Each system was placed in a periodic simulation box and solvated with explicit water molecules. Sodium (Na^+) and chloride (Cl^-) ions were added to neutralize the system and reproduce physiological ionic strength (0.15 M). The simulation protocol included energy minimization, equilibration under constant volume (NVT) and constant pressure (NPT) ensembles, followed by a 100 ns production run at 300 K and 1 bar. Temperature was regulated using the Nosé–Hoover thermostat. A time step of 2 fs was employed. All covalent bonds involving hydrogen atoms were constrained using the SHAKE algorithm. The Particle Mesh Ewald method was used to calculate the electrostatic contribution to non-bonded interactions with a cutoff of 14.0 Å and a time step of 1 fs. The simulation box extended at least 5 Å from the protein surface in all directions. Coordinates were saved every 10 ps.

ISSN 1390-9355
Vol.11. No 3. 2026

Trajectory analysis was performed over the full 100 ns simulation window (10,000 frames). Root mean square deviation (RMSD) was used to monitor global conformational deviations, radius of gyration (Rg) to assess ligand-dependent modulation of overall protein compactness, and root mean square fluctuation (RMSF) as the primary descriptor of residue-level dynamics, particularly within aggregation-prone regions such as the NAC domain and the C-terminal tail. Comparative analyses between ligand-bound complexes and the unbound αSN system were performed to evaluate ligand-dependent effects on conformational heterogeneity relevant to early aggregation processes.

The present computational framework is based on a single aggregation-relevant micelle-bound αSN structure, representing a semi-ordered intermediate between the fully disordered monomeric ensemble and β-sheet-rich aggregates. Although this model does not capture the full conformational heterogeneity of αSN in solution or membrane-bound states, it provides a structurally defined proxy for early aggregation-prone conformations. No ensemble docking, free-energy calculations, or replicate simulations were performed, and the results should therefore be interpreted in a comparative and mechanistic context rather than as quantitative affinity predictions.

Results

Molecular Docking Analysis

Molecular docking analysis revealed marked variability in the interaction propensities of the 38 evaluated compounds toward αSN, reflecting chemically driven and class-dependent binding patterns. Relative docking scores obtained from CB-Dock2, MolDock, Rerank, and PLANTS scoring functions were used exclusively for relative ranking and identification of preferential interaction trends rather than as absolute binding free energy estimates. Table 1 presents the top ten ligands ranked according to their average relative interaction scores across all compounds, highlighting global docking trends independent of chemical classification. The complete docking dataset, including class-specific rankings, is provided in Supplementary Table S1.

Table 1. Top-ranked ligands based on relative docking interaction scores (in kcal/mol).

Ligand	CB-Dock2	MolDock	Rerank	PLANTS	Average score	Key interacting residues
RA (Phenol)	−6.0	−100.66	−82.76	−63.83	−63.31	*HB:* Ser129, Glu126; *HP:* Ala124, Pro128, Gly132, Tyr133, Gln134, Pro138, Glu139, Tyr136, Tyr125
Cur (Phenol)	−5.8	−91.65	−74.02	−56.09	−56.89	*HB:* Ser129; *HP:* Pro128, Glu126,

						Tyr125, Gly132, Tyr136, Tyr133, Gln134, Pro138, Glu139
Mor (Flavonoid)	−5.8	−91.92	−73.75	−61.88	−58.34	HB: Gly132, Pro128; HP: GLN134, Glu131, Ser129, Glu126, Met127, Asp135, Glu130, Tyr133
Mas (Triterpenic acid)	−6.8	−83.75	−63.30	−59.90	−53.44	*HB:* Glu139, Tyr136**;** *HP:* Ala140, Pro138, Gln134, Tyr133, Asp135, Gly132, Glu131, Ser129, Tyr125
HTyr (Phenol)	−4.5	−60.56	−49.47	−53.63	−54.55	*HB:* Gly132, Glu139; *HP:* Pro138, Ala140, Tyr133, Gln134, Glu131
Scu (Flavonoid)	−6.0	−80.22	−62.76	−61.89	−52.72	*HB:* Asp135; *HP:* Ala140, Pro138, Tyr133, Gln134, Gly132, Ser129, Tyr125, Glu126
Ast(Flavonoid)	−6.3	−99.00	−63.71	−40.08	−52.27	*HB:* Asp135, Tyr136, Gly132, Tyr133; *HP:* Glu131, Ser129, Glu126, Tyr125, Glu139, Pro138, Gln134
DHA (Essential fatty acid)	−4.1	−94.25	−56.67	−50.63	−51.41	*HP:* Leu100, Val95, Gly93, Thr92, Lys102, Lys96, Lys97, Phe94
Resv (Phenol)	−5.6	−72.44	−61.38	−58.53	−49.49	*HB:* Tyr136, Asp135; *HP:* Tyr125, Glu126, Gln134, Pro138, Ala140, Gly132, Ser129
α-Hum (Terpene)	−4.8	−63.48	−46.93	−50.63	−41.46	*HP:* Lys45, Val48, Leu38, Lys43, Gly36, Val40, Tyr39

HB: hydrogen bonds; ***HP:*** hydrophobic interactions. Complete docking results for all 38 compounds are provided in **Supplementary Table S1.**

ISSN 1390-9355
Vol.11. No 3. 2026

At a global level, phenolic compounds and flavonoids exhibited the most favorable interaction profiles, followed by triterpenic acids and essential fatty acids. RA, Mor, Cur, and Mas consistently ranked among the top-scoring ligands, with Resv, HTyr, and flavonoids such as Scu and Ast also displaying favorable patterns. Within the terpene class, α-Hum was the highest-ranking compound, outperforming related monoterpenes such as CAR and Thm.

Ligand–protein interaction maps revealed a consistent preference for three aggregation-relevant regions of αSN. The C-terminal region (residues 125–140), frequently targeted by phenols, flavonoids, and triterpenic acids, regulates long-range intramolecular electrostatic interactions that modulate αSN conformation and aggregation propensity. Several ligands also engaged the N-terminal membrane-binding region (residues 32–48), implicated in membrane-associated conformational transitions during early misfolding, and formed hydrophobic contacts in segments adjacent to the NAC domain (residues 92–102), near the aggregation-prone NAC core (residues 61–95). Top-ranked ligands consistently engaged residues such as Ser129, Tyr125, Glu126, Gly132, Gln134, and Tyr136 through hydrogen bonding and hydrophobic interactions, suggesting that binding preferentially modulates regulatory regions rather than inducing global structural stabilization. Class-specific analysis (Supplementary Table S1) revealed scaffold-dependent interaction fingerprints: essential fatty acids displayed moderate propensities, with DHA and IPE the most favorable, binding through hydrophobic contacts with NAC-adjacent residues (92–102). Terpenes exhibited the lowest average scores owing to their small size and lipophilic character, although α-Hum outperformed related monoterpenes and interacted almost exclusively with the N-terminal region.

Triterpenic acids constituted one of the most potent classes, with Mas, Ery, and OA among the top ligands, exhibiting mixed profiles combining hydrogen bonding and extensive hydrophobic contacts across the N-terminal region and C-terminal tail. Phenolic compounds emerged as the most potent class overall: RA and Cur were the two highest-scoring ligands of the dataset, followed by HTyr and Resv, forming extensive hydrogen-bond networks with C-terminal residues including Ser129, Glu126, Gly132, Gln134, Tyr133, Tyr136, Pro138, and Glu139. Flavonoids and isoflavonoids showed similar profiles with slightly lower scores; Mor, Scu, Ast, and EC exhibited dense hydrogen-bond networks involving the C-terminal tail and NAC-adjacent regions. Alkaloids and clinically used drugs showed moderate propensities, with Mel the highest-ranking and displaying a mixed pattern centered on the C-terminal region.

Collectively, these results establish a scaffold-dependent hierarchy of αSN interaction mechanisms: lipophilic scaffolds such as terpenes and fatty acids preferentially target the N-terminal membrane-interacting region and NAC-adjacent hydrophobic interfaces, whereas polyphenols, flavonoids, and

ISSN 1390-9355
Vol.11. No 3. 2026

triterpenic acids engage the C-terminal regulatory tail through extensive hydrogen-bond networks. Based on class-specific ranking, the ligand with the highest average docking score within each class was selected as a representative compound for subsequent MD simulations, enabling mechanistic comparison while avoiding redundancy among structurally related molecules. Predicted binding modes of representative ligands are shown in Figure 1.

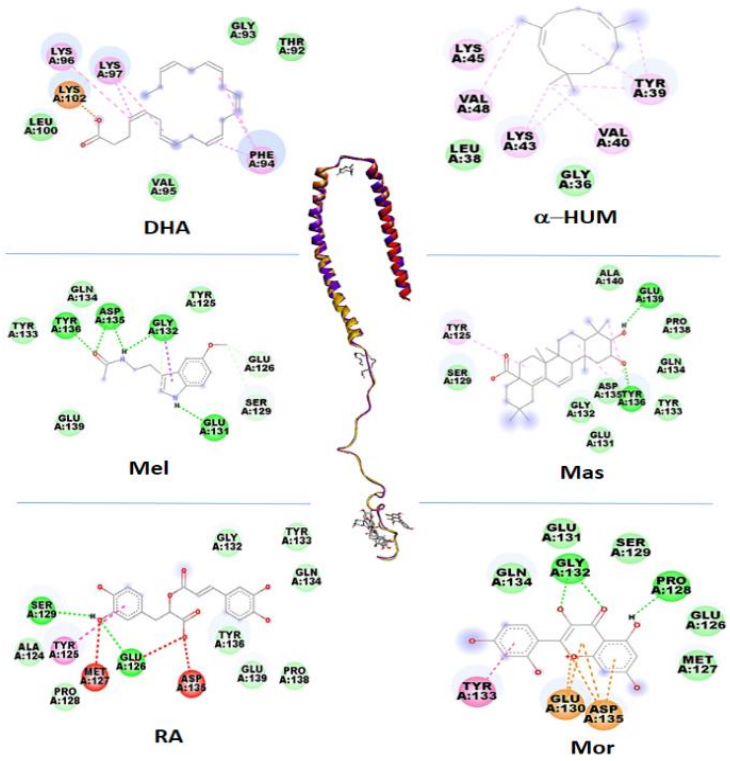


Figure 1. Predicted binding sites of representative ligands with the highest average docking score within each chemical class on α-synuclein. These ligands were selected for subsequent molecular dynamics simulations and illustrate class-specific interaction patterns targeting aggregation-relevant regions, including the C-terminal tail, N-terminal membrane-binding domain, and NAC-adjacent segments. DHA (Docosahexaenoic acid); Mas (Maslinic acid); RA (Rosmarinic acid); Mor (Morin); α-Hum (α-Humulene); Mel (Melatonin).

Molecular Dynamics Analysis: Stability and Flexibility of the Complexes

To assess the dynamic consequences of ligand association, trajectories were analyzed over the full 100 ns simulation window using RMSD, R_g, and RMSF as complementary descriptors of global and local conformational behavior (Figure 2).

The unbound αSN system exhibited an average RMSD of approximately 2.7 Å, consistent with the conformational heterogeneity expected for intrinsically disordered proteins. Among ligand-bound systems, Mas displayed the lowest RMSD (~2.4 Å), whereas DHA exhibited higher RMSD values

ISSN 1390-9355
Vol.11. No 3. 2026

(~3.4 Å), indicating enhanced global fluctuations. Mel and α-Hum showed RMSD values comparable to the unbound protein (~2.9 Å), while RA and Mor displayed higher RMSD values (3.2–3.3 Å) despite favorable docking scores. RMSD trajectories for all systems plateaued after approximately 90 ns, indicating convergence toward stable conformational ensembles. The unbound αSN ensemble displayed an average R_g of approximately 2.8 nm, reflecting its predominantly extended conformational landscape.

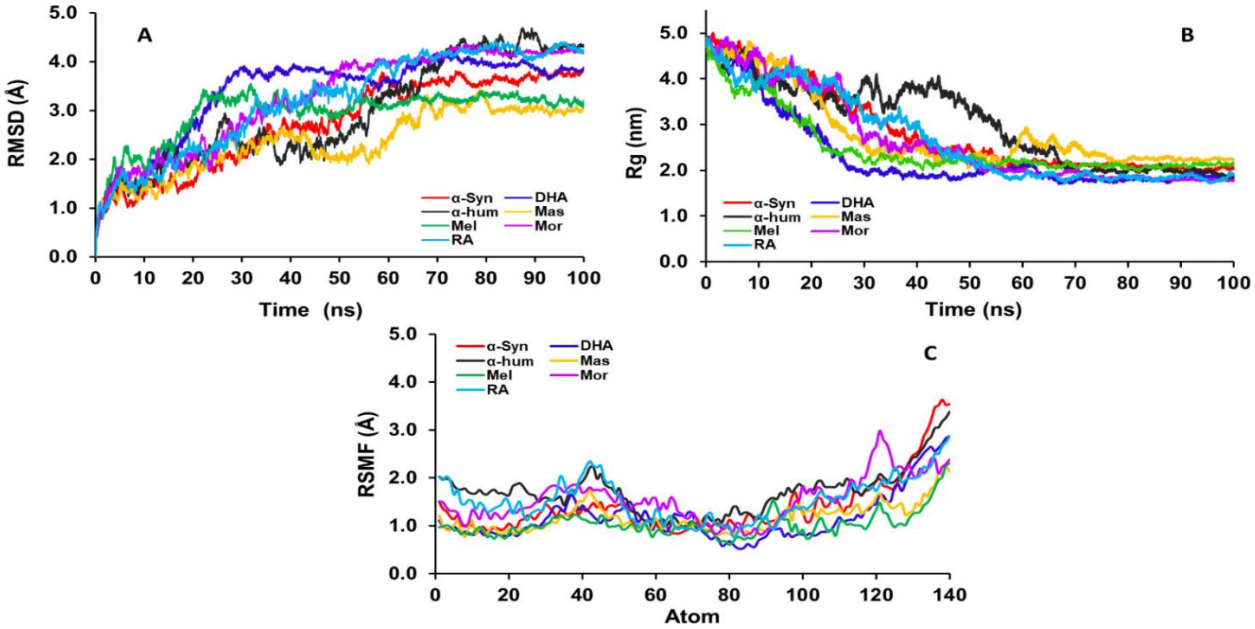


Figure 2. Conformational dynamics of αSN in the unbound state and in complex with selected ligands over a 100 ns molecular dynamics trajectory (10,000 frames). (A) Root mean square deviation (RMSD) illustrating global conformational deviations over time. (B) Radius of gyration (R_g) describing changes in overall protein compactness, which are not interpreted as direct indicators of conformational stability for this intrinsically disordered protein. (C) Root mean square fluctuation (RMSF) highlighting ligand-dependent modulation of residue-level flexibility across the αSN sequence, particularly in aggregation-relevant regions. DHA (Docosahexaenoic acid); Mas (Maslinic acid); RA (Rosmarinic acid); Mor (Morin); α-Hum (α-Humulene); Mel (Melatonin).

Ligand binding induced compound-specific effects on compactness. DHA promoted the most compact ensemble ($R_g \approx 2.3$ nm), Mel induced modest compaction ($R_g \approx 2.5$ nm), whereas α-Hum slightly increased the average R_g (~3.0 nm). RA and Mor produced minimal changes relative to the unbound state. R_g trajectories stabilized after approximately 70 ns.

Residue-level flexibility analysis revealed ligand-specific modulation of local dynamics along the αSN sequence. Mel and Mas induced the most pronounced reductions in RMSF, particularly within aggregation-prone regions including the NAC domain. DHA also reduced RMSF values despite

higher global RMSD, indicating localized stabilization. In contrast, α-Hum, RA, and Mor produced only modest reductions in residue-level flexibility.

Together, these results demonstrate that ligand binding produces heterogeneous and scaffold-dependent effects on αSN conformational dynamics. RMSF emerged as the most informative descriptor for evaluating ligand-induced modulation of aggregation-relevant regions, whereas RMSD and R_g primarily reflected ensemble-level behavior. The convergence of RMSD and R_g trajectories confirms that all systems reached stable conformational ensembles within the simulation timeframe, supporting the robustness of the comparative dynamic analyses.

Discussion

Ligand-Responsive Regions of α-Synuclein and Aggregation-Relevant Interfaces

The present study demonstrates that αSN contains multiple ligand-responsive regions that can be selectively engaged by chemically diverse bioactive compounds. Integration of docking-based interaction ranking with molecular dynamics analysis indicates that aggregation-relevant behavior is not governed by a single dominant binding hotspot, but rather by the coordinated modulation of multiple regulatory interfaces whose relative contribution depends on ligand scaffold, interaction mode, and dynamic context.

These findings are consistent with accumulating experimental and computational evidence showing that natural and synthetic compounds modulate αSN aggregation by binding to defined protein segments and reshaping its conformational ensemble.[4,34-36] Polyphenols, flavonoids, and isoflavonoids have been shown to reduce αSN fibrillation and cellular toxicity by stabilizing less aggregation-prone conformations.[37,38]

Although the micelle-bound αSN structure represents a simplified proxy that does not fully capture the heterogeneous conformational ensemble of αSN in solution, this semi-folded state has been extensively employed to model early aggregation-prone conformations and ligand-accessible regulatory surfaces.[39–42] It represents a structurally defined interm ediate between the fully disordered monomer and β-sheet-rich aggregates and captures early α-helical rearrangements that precede pathogenic misfolding.

Docking analysis identified several natural compounds—particularly RA, Mor, Cur, Mas, and α-Hum—as preferential binders to regions previously implicated in aggregation control. Across chemical classes, three recurrent interaction regions were consistently observed: the C-terminal tail (residues 124–140), the N-terminal membrane-interacting region, and a hydrophobic segment

ISSN 1390-9355
Vol.11. No 3. 2026

adjacent to the NAC domain. These regions overlap with surfaces known to regulate αSN conformational equilibria, membrane association, and fibrillation kinetics.[41–46]

This targeting pattern agrees with NMR studies showing that aggregation inhibitors bind defined αSN segments, particularly residues 3–18 and 38–51, and that aromatic scaffolds and polar functional groups favor these interactions.[47,48] In silico studies further demonstrate that ligands engage specific αSN interfaces and modulate conversion into amyloidogenic conformations.[49–51]

The C-terminal region, preferentially targeted by phenolic compounds and flavonoids, plays a critical autoinhibitory role by maintaining long-range electrostatic contacts with the NAC domain. Ligands such as RA and Mor formed extensive hydrogen-bond networks with residues including Ser129, Tyr125, Glu126, Gly132, Gln134, and Tyr136, consistent with reinforcement of this intrinsic regulatory function. This behavior agrees with experimental evidence showing that polyphenols and flavonoids inhibit nucleation and redirect fibril formation toward less toxic species.[37, 52–54]

In contrast, triterpenic acids and terpenes predominantly engaged hydrophobic residues within the N-terminal and NAC-adjacent regions. Binding in the N-terminal domain may modulate membrane-induced conformational rearrangements that precede pathological aggregation, while binding near NAC-adjacent surfaces may sterically interfere with nucleation-prone interfaces, potentially limiting early β-sheet formation or oligomer growth. Similar mechanisms have been proposed for small molecules targeting these αSN regions[55–57] and for plant-derived terpenoids and phenolic compounds stabilizing less aggregation-prone conformations.[58,59]

Integrating Docking and Molecular Dynamics: Dynamic Stability and Residue-Level Modulation

While molecular docking delineated preferential interaction patterns across aggregation-relevant regions of αSN, MD simulations provide essential context regarding the dynamic behavior of these complexes. All ligand–protein systems formed dynamically stable conformational ensembles over the 100 ns simulation timeframe, as evidenced by RMSD and Rg trajectories converging toward equilibrated states. Differences among ligands therefore reflect functional variation within stable ensembles rather than destabilization or dissociation.

These observations are consistent with previous MD studies showing that ligand binding modulates the αSN conformational landscape and influences transitions toward amyloidogenic states [60]. Moreover, interaction of αSN with lipids and membrane-mimetic environments induces substantial conformational rearrangements that affect aggregation and toxicity,[61, 62] supporting the relevance of dynamic descriptors for evaluating ligand-induced modulation.

ISSN 1390-9355
Vol.11. No 3. 2026

Across all systems, RMSD plateaued after approximately 90 ns and Rg stabilized after approximately 70 ns, confirming equilibration. Within this framework, ligand-specific modulation of global and local dynamics was observed. Mel exhibited intermediate RMSD (~2.9 Å), moderate compaction (R_g ~2.5 nm), and the lowest RMSF (~1.0 Å), indicating pronounced residue-level stabilization. Mas showed lower RMSD (~2.4 Å) and reduced RMSF (~1.2 Å), consistent with combined global and local stabilization. DHA displayed higher RMSD (~3.4 Å) but reduced RMSF (~1.2 Å) and increased compactness (R_g ~2.3 nm), indicating selective stabilization of aggregation-relevant regions despite enhanced global fluctuations, in agreement with studies implicating essential fatty acids in αSN homeostasis.[55, 60]

In contrast, RA and Mor—despite strong docking scores—exhibited higher RMSD values (3.2–3.3 Å), modest reductions in RMSF (1.5–1.6 Å), and minimal changes in Rg, underscoring that high static interaction propensity does not necessarily translate into dynamic stabilization in intrinsically disordered proteins. α-Hum showed limited global effects but selectively dampened flexibility in NAC-adjacent regions, highlighting localized modulation of nucleation-prone interfaces.

Collectively, these results indicate that RMSF constitutes the most informative descriptor of functional modulation in αSN, whereas RMSD and Rg primarily reflect ensemble equilibration and global conformational behavior. This pattern is consistent with experimental observations that phytochemicals influence amyloidogenic pathways primarily through local conformational effects rather than global folding.[63–65]

Mechanistic Implications and Hierarchical Modulation of Aggregation-Relevant Conformational States

By integrating class-specific docking trends with molecular dynamics–derived conformational descriptors, the present study supports a hierarchical and multimodal computational framework for modulation of αSN aggregation-relevant conformational states. This framework reflects the multifactorial nature of synucleinopathies, in which oxidative stress, neuroinflammation, mitochondrial dysfunction, and proteostasis collapse converge to promote pathological conformational transitions, NAC domain exposure, oligomer nucleation, and amyloid propagation.[1, 2, 7, 9, 66, 67]

Rather than acting as classical inhibitors, most bioactive compounds identified here are better interpreted as conformational modulators that reshape the αSN ensemble toward less aggregation-prone states. This interpretation is consistent with experimental data showing that natural and synthetic compounds inhibit primary nucleation, stabilize non-toxic oligomers, or redirect fibril formation toward less cytotoxic species.[52–54]

Within this context, two complementary and non-mutually exclusive mechanistic models emerge. The first involves stabilization of non-aggregating conformational ensembles through local reduction of residue-level flexibility in aggregation-relevant regions, particularly within the NAC domain and the membrane-interacting N-terminal segment. This mechanism is supported by reduced RMSF values observed for ligands such as Mel, Mas, and DHA and is consistent with reports that multifunctional compounds inhibit αSN aggregation and protect against αSN-induced neurotoxicity in cellular and animal models.[68–71]

The second model entails steric and surface-level interference with early aggregation events. In this scenario, ligands occupying NAC-adjacent segments or hydrophobic interfaces hinder monomer addition and oligomer growth by masking nucleation-prone surfaces rather than stabilizing a compact monomeric fold. This behavior is particularly evident for hydrophobic scaffolds such as terpenes and triterpenic acids and is consistent with studies reporting high-affinity binding of plant-derived terpenoids and phenols to αSN and stabilization of conformations less prone to aggregation.[58, 72–74]

The structural diversity of the evaluated compounds and their scaffold-dependent interaction patterns support a stratified modulation model in which chemically distinct ligands converge on complementary stages of the αSN aggregation cascade.[75,76] Essential fatty acids primarily modulate membrane-associated conformations and global compactness, polyphenols and flavonoids preferentially engage C-terminal regulatory segments and NAC-flanking regions, triterpenic acids combine cytoprotective signaling with direct engagement of regulatory surfaces, whereas terpenes primarily target hydrophobic N-terminal interfaces. Alkaloids and clinically used drugs exhibit mixed hydrogen-bonding and peripheral hydrophobic interactions.

Figure 3 integrates these class-specific docking interaction patterns with MD-based functional interpretation, illustrating how chemically diverse ligands converge on complementary modulation points along the αSN aggregation cascade. This scheme is intended as a conceptual synthesis rather than a definitive mechanistic map.

ISSN 1390-9355
Vol.11. No 3. 2026

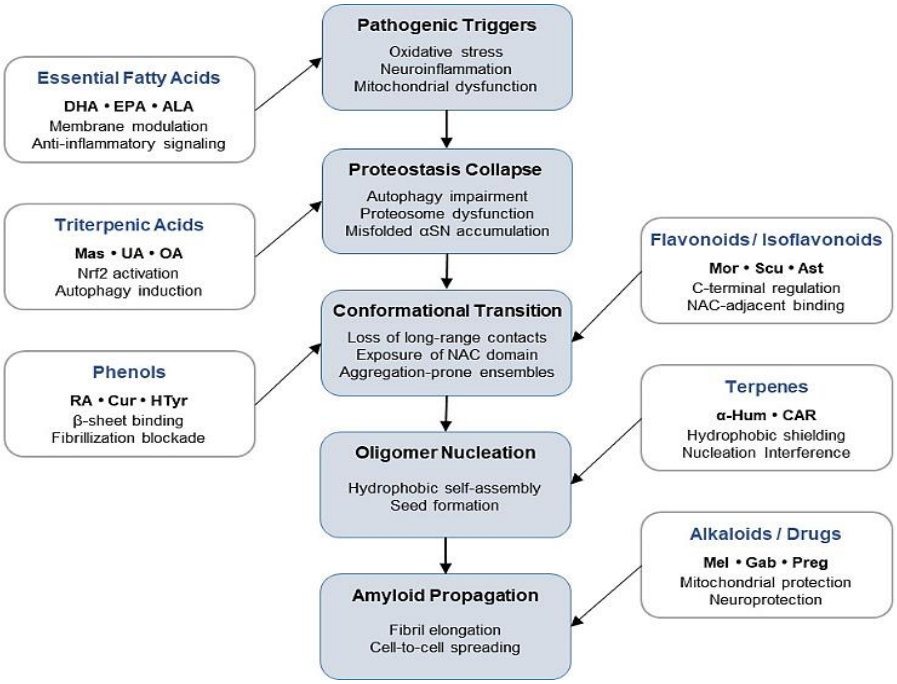


Figure 3. Multimodal strategy targeting α-synuclein aggregation. Conceptual framework integrating class-specific docking patterns (Supplementary Table S1) with molecular dynamics–derived functional insights. Diverse ligands converge on complementary points along the α-synuclein pathological cascade, including modulation of membrane-associated conformations, redox/inflammatory environment, conformational dynamics, early hydrophobic self-assembly, and β-sheet fibrillization. The scheme illustrates a hierarchical, multimodal computational approach to modulate α-synuclein aggregation. DHA (Docosahexaenoic acid); EPA (Eicosapentaenoic acid); ALA (Linolenic acid); Mas (Maslinic acid); UA (Ursolic Acid); OA (Oleanolic acid); RA (Rosmarinic acid); Cur (Curcumin); Htyr (Hydroxytyrosol); Mor (Morin); Scu (Scutellarein); Ast (Astragalin); α-Hum (α-Humulene); CAR (Carvacrol); (Mel (Melatonin); Gab (Gabapentin); Preg (Pregabalin).

Collectively, these findings indicate that effective computational modulation of αSN aggregation cannot be inferred from docking scores alone. While RMSD and Rg convergence confirm dynamic stability of ligand-bound ensembles, RMSF provides critical insight into functional modulation at aggregation-relevant regions. This integrative framework supports the prioritization of structurally diverse bioactive scaffolds, and potentially rational combinations thereof, for experimental validation and further exploration of aggregation-modulating conformational mechanisms.

ISSN 1390-9355
Vol.11. No 3. 2026

Conclusions

This study establishes an integrative computer-aided drug design framework for characterizing scaffold-dependent interaction patterns and conformational modulation mechanisms of αSN, an intrinsically disordered protein whose aggregation-prone conformational transitions underlie the early stages of Parkinson's disease and related synucleinopathies. By combining comprehensive blind molecular docking with class-based molecular dynamics simulations, the results demonstrate that αSN aggregation-relevant behavior is governed by coordinated engagement of multiple regulatory interfaces rather than a single dominant binding site.

Docking analyses revealed that chemically diverse ligands preferentially interact with key aggregation-relevant regions of αSN, including NAC-adjacent segments, the N-terminal membrane-interacting domain, and the C-terminal regulatory tail. Representative ligands selected by class-specific docking performance were subjected to molecular dynamics simulations, which showed that all ligand–protein systems form dynamically stable conformational ensembles, with RMSD and radius of gyration trajectories converging after approximately 70–90 ns, confirming equilibration of the sampled conformational space.

Within this equilibrated framework, ligand-dependent modulation of residue-level flexibility revealed distinct functional signatures. Mel, DHA, and Mas were associated with reduced RMSF values in aggregation-prone regions, consistent with localized stabilization of non-aggregating ensembles. Hydrophobic compounds such as α-humulene selectively dampened flexibility at nucleation-prone interfaces without inducing global compaction, whereas polyphenols such as RA and Mor primarily engaged C-terminal regulatory regions with more limited effects on overall flexibility. These findings reinforce that static docking affinity alone is insufficient to predict functional modulation in intrinsically disordered proteins, and that residue-level dynamic descriptors provide a more informative basis for evaluating aggregation-relevant conformational behavior.

Collectively, the results support a multifaceted computational model in which polyphenols, flavonoids, terpenes, triterpenic acids, and unsaturated fatty acids modulate αSN aggregation through complementary mechanisms, including stabilization of non-amyloidogenic ensembles, steric interference at nucleation interfaces, and modulation of membrane-associated conformational transitions—consistent with epidemiological evidence linking polyphenol- and terpene-rich dietary patterns to reduced PD risk. Overall, these insights provide a mechanistically grounded basis for prioritizing natural compounds and chemical scaffolds—individually or in rational combinations—for subsequent experimental validation and further exploration of aggregation-modulating conformational mechanisms.

Supplementary Material: The following are available online at www.revistabionatura.com/xxx/s1, Table S1. Relative binding energies (in kcal/mol) obtained from molecular docking.

Author Contributions: YQ: Investigation, Methodology, Writing – original draft, Writing – review and editing, Conceptualization. AD: Investigation, Writing – review and editing, MM: Investigation, AV: Methodology, AM: Methodology, YB: Investigation, LGP: Conceptualization, YJA.: Writing – review and editing. All authors have read and agreed to the published version of the manuscript.

Funding: This research received no external funding.

Institutional Review Board Statement: Not applicable.

Conflicts of Interest: The authors declare no conflict of interest.

References

1. Calabresi P, Di Lazzaro G, Marino G, Campanelli F, Ghiglieri V. Advances in Understanding the Function of Alpha-Synuclein: Implications for Parkinson's Disease. Brain. 2023;46(9):3587–3597. https://doi.org/10.1093/brain/awad150
2. Morris HR, Spillantini MG, Sue CM, Williams-Gray CH. The Pathogenesis of Parkinson's Disease. Lancet. 2024;403(10423):293–304. https://doi.org/10.1016/S0140-6736(23)01478-2
3. Spillantini MG, Schmidt ML, Lee VM, Trojanowski JQ, Jakes R, Goedert M. α-Synuclein in Lewy Bodies. Nature. 1997;388(6645):839–840. https://doi.org/10.1038/42166
4. da Silva IJS, da Silva MF, de Assis Dutra TS, de Souza SO, de Araújo-Júnior JX, Leite ACR, da Silva Rodrigues EE, da Silva-Júnior EF. Alpha-Synuclein Aggregation in Parkinson's Disease. Adv Protein Chem Struct Biol. 2025;146:35–75. https://doi.org/10.1016/bs.apcsb.2024.11.002
5. Paulėkas E, Vanagas T, Lagunavičius S, Pajėdienė E, Petrikonis K, Rastenytė D. Navigating the Neurobiology of Parkinson's: The Impact and Potential of α-Synuclein. Biomedicines. 2024;12(9):2121. https://doi.org/10.3390/biomedicines12092121
6. Flagmeier P, Meisl G, Vendruscolo M, Knowles T, Dobson C, Buell A, Galvagnion C. Mutations Associated with Familial Parkinson's Disease Alter the Initiation and Amplification Steps of α-Synuclein Aggregation. Proc Natl Acad Sci U S A. 2016;113(37):10328–10333. https://doi.org/10.1073/pnas.1604645113
7. Forloni G. Alpha Synuclein: Neurodegeneration and Inflammation. Int J Mol Sci. 2023;24(6):5914. https://doi.org/10.3390/ijms24065914
8. Henriques A, Rouvière L, Giorla E, Farrugia C, El Waly B, Poindron P, Callizot N. Alpha-Synuclein: The Spark That Flames Dopaminergic Neurons, in Vitro and in Vivo Evidence. Int J Mol Sci. 2022;23(17):9864. https://doi.org/10.3390/ijms23179864

9. Cardinale A, Calabrese V, De Iure A, Picconi B. Alpha-Synuclein as a Prominent Actor in the Inflammatory Synaptopathy of Parkinson's Disease. Int J Mol Sci. 2021;22(12):6517. https://doi.org/10.3390/ijms22126517
10. Saramowicz K, Siwecka N, Galita G, Kucharska-Lusina A, Rozpędek-Kamińska W, Majsterek I. Alpha-Synuclein Contribution to Neuronal and Glial Damage in Parkinson's Disease. Int J Mol Sci. 2024;25(1):360. https://doi.org/10.3390/ijms25010360
11. Longhena F, Faustini G, Spillantini M, Bellucci A. Living in Promiscuity: The Multiple Partners of Alpha-Synuclein at the Synapse in Physiology and Pathology. Int J Mol Sci. 2019;20(1):141. https://doi.org/10.3390/ijms20010141
12. Ulmer T, Bax A, Cole N, Nussbaum R. Structure and Dynamics of Micelle-Bound Human α-Synuclein. J Biol Chem. 2005;280(10):9595–9603. https://doi.org/10.1074/jbc.M411805200
13. Salmaso V, Moro S. Bridging Molecular Docking to Molecular Dynamics in Exploring Ligand-Protein Recognition Process: An Overview. Front Pharmacol. 2018;9:923. https://doi.org/10.3389/fphar.2018.00923
14. Yu J, Lyubchenko Y. Early Stages for Parkinson's Development: α-Synuclein Misfolding and Aggregation. J Neuroimmune Pharmacol. 2009;4(1):10–16. https://doi.org/10.1007/s11481-008-9115-5
15. Bisaglia M. Mediterranean Diet and Parkinson's Disease. Int J Mol Sci. 2023;24(1):42. https://doi.org/10.3390/ijms24010042
16. Metcalfe-Roach A, Yu AC, Golz E, Cirstea M, Sundvick K, Kliger D, Foulger LH, Mackenzie M, Finlay BB, Appel-Cresswell S. MIND and Mediterranean Diets Associated with Later Onset of Parkinson's Disease. Mov Disord. 2021;36(4):977–984. https://doi.org/10.1002/mds.28464
17. Molsberry S, Bjornevik K, Hughes K, Healy B, Schwarzschild M, Ascherio A. Diet Pattern and Prodromal Features of Parkinson Disease. Neurology. 2020;95(15):e2095–e2108. https://doi.org/10.1212/WNL.0000000000010523
18. Hussain G, Zhang L, Rasul A, Anwar H, Sohail MU, Razzaq A, Aziz N, Shabbir A, Ali M, Sun T. Role of Plant-Derived Flavonoids and Their Mechanism in Attenuation of Alzheimer's and Parkinson's Diseases: An Update of Recent Data. Molecules. 2018;23(4):814. https://doi.org/10.3390/molecules23040814
19. Shah S, Duda J. Dietary Modifications in Parkinson's Disease: A Neuroprotective Intervention? Med Hypotheses. 2015;85(6):1002–1005. https://doi.org/10.1016/j.mehy.2015.08.018
20. Merghany RM, El-Sawi SA, Naser AFA, Ezzat SM, Moustafa SFA, Meselhy MR. A Comprehensive Review of Natural Compounds and Their Structure–Activity Relationship in

Parkinson's Disease: Exploring Potential Mechanisms. Naunyn Schmiedebergs Arch Pharmacol. 2025;398(3):2229–2258. https://doi.org/10.1007/s00210-024-03462-4

21. Puri V, Kanojia N, Sharma A, Huanbutta K, Dheer D, Sangnim T. Natural Product-Based Pharmacological Studies for Neurological Disorders. Front Pharmacol. 2022;13:1011740. https://doi.org/10.3389/fphar.2022.1011740
22. Ko J, Park H, Heo L, Seok C. GalaxyWEB Server for Protein Structure Prediction and Refinement. Nucleic Acids Res. 2012;40(W1):W294–W297. https://doi.org/10.1093/nar/gks493
23. Williams CJ, Headd JJ, Moriarty NW, Prisant MG, Videau LL, Deis LN, Verma V, Keedy DA, Hintze BJ, Chen VB, Jain S, Lewis SM, Arendall WB 3rd, Snoeyink J, Adams PD, Lovell SC, Richardson JS, Richardson DC. MolProbity: More and Better Reference Data for Improved All-Atom Structure Validation. Protein Sci. 2018;27(1):293–315. https://doi.org/10.1002/pro.3330
24. Kim S, Chen J, Cheng T, Gindulyte A, He J, He S, Li Q, Shoemaker BA, Thiessen PA, Yu B, Zaslavsky L, Zhang J, Bolton EE. PubChem 2023 Update. Nucleic Acids Res. 2023;51(D1):D1373–D1380. https://doi.org/10.1093/nar/gkac956
25. Hanwell M, Curtis D, Lonie D, Vandermeersch T, Zurek E, Hutchison G. Avogadro: An Advanced Semantic Chemical Editor, Visualization, and Analysis Platform. J Cheminform. 2012;4(1):17. https://doi.org/10.1186/1758-2946-4-17
26. Bitencourt-Ferreira G, de Azevedo W. Molegro Virtual Docker for Docking. In: Docking Screens for Drug Discovery. New York: Springer; 2019. p. 149–167. https://doi.org/10.1007/978-1-4939-9752-7_10
27. Korb O, Stützle T, Exner T. Empirical Scoring Functions for Advanced Protein–Ligand Docking with PLANTS. J Chem Inf Model. 2009;49(1):84–96. https://doi.org/10.1021/ci800298z
28. Thomsen R, Christensen M. MolDock: A New Technique for High-Accuracy Molecular Docking. J Med Chem. 2006;49(11):3315–3321. https://doi.org/10.1021/jm051197e
29. Baroroh S, Muscifa Z, Destiarani W, Rohmatullah F, Yusuf M. Molecular Interaction Analysis and Visualization of Protein-Ligand Docking Using Biovia Discovery Studio Visualizer. Int J Curr Biotechnol. 2023;2(1):22–29. https://doi.org/10.24198/ijcb.v2i1.46322
30. Liu Y, Yang X, Gan J, Chen S, Xiao Z, Cao Y. CB-Dock2: Improved Protein–Ligand Blind Docking by Integrating Cavity Detection, Docking and Homologous Template Fitting. Nucleic Acids Res. 2022;50(W1):W159–W164. https://doi.org/10.1093/nar/gkac394
31. Yang X, Liu Y, Gan J, Xiao ZX, Cao Y. FitDock: Protein–Ligand Docking by Template Fitting. Brief Bioinform. 2022;23(3):bbac087. https://doi.org/10.1093/bib/bbac087
32. Kasahara K, Terazawa H, Itaya H, Goto S, Nakamura H, Takahashi T, Higo J. myPresto/omegagene 2020: A Molecular Dynamics Simulation Engine for Virtual-System

Coupled Sampling. Biophys Physicobiol. 2020;17:140–146. https://doi.org/10.2142/biophysico.BSJ-2020013

33. Alvarado Y, Olivarez Y, Lossada C, Vera-Villalobos J, Paz J, Vera E, Loroño M, Vivas A, Torres F, Jeffreys L, Hurtado-León M, González-Paz L. Interaction of the New Inhibitor Paxlovid (PF-07321332) and Ivermectin with the Monomer of the Main Protease SARS-CoV-2: A Volumetric Study Based on Molecular Dynamics, Elastic Networks, Classical Thermodynamics and SPT. Comput Biol Chem. 2022;99:107692. https://doi.org/10.1016/j.compbiolchem.2022.107692
34. Mohammad-Beigi H, Aliakbari F, Sahin C, Lomax C, Tawfike A, Schafer NP, Amiri-Nowdijeh A, Eskandari H, Møller IM, Hosseini-Mazinani M, Christiansen G, Ward JL, Morshedi D, Otzen DE. Oleuropein Derivatives from Olive Fruit Extracts Reduce α-Synuclein Fibrillation and Oligomer Toxicity. J Biol Chem. 2019;294(11):4215–4232. https://doi.org/10.1074/jbc.RA118.005723
35. Farzadfard A, König A, Petersen S, Nielsen J, Vasili E, Dominguez-Meijide A, Buell A, Outeiro T, Otzen D. Glycation Modulates Alpha-Synuclein Fibrillization Kinetics: A Sweet Spot for Inhibition. J Biol Chem. 2022;298(5):101848. https://doi.org/10.1016/j.jbc.2022.101848
36. Andersen C, Grønnemose A, Pedersen J, Nowak J, Christiansen G, Nielsen J, Mulder F, Otzen D, Jørgensen T. Lipid Peroxidation Products HNE and ONE Promote and Stabilize Alpha-Synuclein Oligomers by Chemical Modifications. Biochemistry. 2021;60(48):3643–3658. https://doi.org/10.1021/acs.biochem.1c00478
37. Braun AR, Liao EE, Horvath M, Kalra P, Acosta K, Young MC, Kochen NN, Lo CH, Brown R, Evans MD, Pomerantz WCK, Rhoades E, Luk K, Cornea RL, Thomas DD, Sachs JN. Potent Inhibitors of Toxic Alpha-Synuclein Identified via Cellular Time-Resolved FRET Biosensors. NPJ Parkinsons Dis. 2021;7(1):52. https://doi.org/10.1038/s41531-021-00195-6
38. Andersen C, Yoshimura Y, Nielsen J, Otzen D, Mulder F. How Epigallocatechin Gallate Binds and Assembles Oligomeric Forms of Human Alpha-Synuclein. J Biol Chem. 2021;296:100788. https://doi.org/10.1016/j.jbc.2021.100788
39. Gul G. In Silico Screening of Peptide Inhibitors Targeting α-Synuclein for Parkinson's Disease. J Mol Graph Model. 2025;134:109079. https://doi.org/10.1016/j.jmgm.2025.109079
40. Chakraborty G, Patra N. Elucidating the Molecular Basis of 14-3-3 Interaction with α-Synuclein: Insights from Molecular Dynamics Simulations and the Design of a Novel Protein–Protein Interaction Inhibitor. J Phys Chem B. 2024;128(29):7068–7085. https://doi.org/10.1021/acs.jpcb.4c01743

41. Rezaei M, Jahanbin J, Rastkar A. The Interaction of Curcumin and Rosmarinic Acid with Non-Amyloid-Component Domain of Alpha-Synuclein: A Molecular Dynamics Study. ChemistrySelect. 2020;5(11):3312–3320. https://doi.org/10.1002/slct.201904799
42. Davidson W, Jonas A, Clayton D, George J. Stabilization of α-Synuclein Secondary Structure upon Binding to Synthetic Membranes. J Biol Chem. 1998;273(16):9443–9449. https://doi.org/10.1074/jbc.273.16.9443
43. Bussell R, Eliezer D. A Structural and Functional Role for 11-Mer Repeats in α-Synuclein and Other Exchangeable Lipid Binding Proteins. J Mol Biol. 2003;329(4):763–778. https://doi.org/10.1016/S0022-2836(03)00520-5
44. Michell A, Luheshi L, Barker R. Skin and Platelet α-Synuclein as Peripheral Biomarkers of Parkinson's Disease. Neurosci Lett. 2005;381(3):294–298. https://doi.org/10.1016/j.neulet.2005.02.030
45. Dedmon M, Lindorff-Larsen K, Christodoulou J, Vendruscolo M, Dobson C. Mapping Long-Range Interactions in α-Synuclein Using Spin-Label NMR and Ensemble Molecular Dynamics Simulations. J Am Chem Soc. 2005;127(2):476–477. https://doi.org/10.1021/ja044834j
46. Bertoncini C, Jung Y, Fernandez C, Hoyer W, Griesinger C, Jovin T, Zweckstetter M. Release of Long-Range Tertiary Interactions Potentiates Aggregation of Natively Unstructured α-Synuclein. Proc Natl Acad Sci U S A. 2005;102(5):1430–1435. https://doi.org/10.1073/pnas.0407146102
47. Buratti FA, Boeffinger N, Garro HA, Flores JS, Hita FJ, Gonçalves PDC, Copello FDR, Lizarraga L, Rossetti G, Carloni P, Zweckstetter M, Outeiro TF, Eimer S, Griesinger C, Fernández CO. Aromaticity at Position 39 in α-Synuclein: A Modulator of Amyloid Fibril Assembly and Membrane-Bound Conformations. Protein Sci. 2022;31(7):e4360. https://doi.org/10.1002/pro.4360
48. Rao J, Dua V, Ulmer T. Characterization of α-Synuclein Interactions with Selected Aggregation-Inhibiting Small Molecules. Biochemistry. 2008;47(16):4651–4656. https://doi.org/10.1021/bi8002378
49. Sahihi M, Gaci F, Navizet I. Identification of New Alpha-Synuclein Fibrillogenesis Inhibitor Using in Silico Structure-Based Virtual Screening. J Mol Graph Model. 2021;108:108010. https://doi.org/10.1016/j.jmgm.2021.108010
50. Saffari B, Amininasab M. Crocin Inhibits the Fibrillation of Human α-Synuclein and Disassembles Mature Fibrils: Experimental Findings and Mechanistic Insights from Molecular Dynamics Simulation. ACS Chem Neurosci. 2021;12(20):3913–3927. https://doi.org/10.1021/acschemneuro.1c00379

51. Sangwan S, Sahay S, Murray K, Morgan S, Guenther E, Jiang L, Williams C, Vinters H, Goedert M, Eisenberg D. Inhibition of Synucleinopathic Seeding by Rationally Designed Inhibitors. eLife. 2020;9:e46775. https://doi.org/10.7554/eLife.46775
52. Basellini MJ, Granadino-Roldán JM, Torres-Ortega PV, Simmini G, Rubio-Martinez J, Marin S, Cappelletti G, Cascante M, Cañuelo A. Oleuropein Aglycone, an Olive Polyphenol, Influences Alpha-Synuclein Aggregation and Exerts Neuroprotective Effects in Different Parkinson's Disease Models. Mol Neurobiol. 2025;62(12):15741–15758. https://doi.org/10.1007/s12035-025-05208-6
53. Naitė I, Mikalauskaitė K, Paulauskaitė M, Sniečkutė R, Smirnovas V, Brukštus A, Žiaunys M, Žutautė I. Imidazo[2,1-b][1,3]thiazine Derivatives as Potential Modulators of Alpha-Synuclein Amyloid Aggregation. ACS Chem Neurosci. 2024;15(24):4418–4430. https://doi.org/10.1021/acschemneuro.4c00451
54. Ahanger I, Dar T. Small Molecule Modulators of Alpha-Synuclein Aggregation and Toxicity: Pioneering an Emerging Arsenal against Parkinson's Disease. Ageing Res Rev. 2024;101:102538. https://doi.org/10.1016/j.arr.2024.102538
55. El-Agnaf O, Jakes R, Curran M, Middleton D, Ingenito R, Bianchi E, Pessi A, Neill D, Wallace A. Aggregates from Mutant and Wild-Type α-Synuclein Proteins and NAC Peptide Induce Apoptotic Cell Death in Human Neuroblastoma Cells by Formation of β-Sheet and Amyloid-Like Filaments. FEBS Lett. 1998;440(1-2):71–75. https://doi.org/10.1016/S0014-5793(98)01418-5
56. Giasson B, Murray I, Trojanowski J, Lee V. A Hydrophobic Stretch of 12 Amino Acid Residues in the Middle of α-Synuclein Is Essential for Filament Assembly. J Biol Chem. 2001;276(4):2380–2386. https://doi.org/10.1074/jbc.M008919200
57. Das V, Modarres Mousavi SM, Annadurai N, Sukur S, Mehrnejad F, Moradi S, Malina L, Kolaříková M, Ranc V, Frydrych I, Kouřil R, Hosseinkhani S, Hajdúch M, Nikkhah M. Hydrophobic Residues in the α-Synuclein NAC Domain Drive Seed-Competent Fibril Formation and Are Targeted by Peptide Inhibitors. FEBS J. 2026;293(1):134–155. https://doi.org/10.1111/febs.70222
58. Bhattacharya S, Gupta N, Dutta A, Khanra PK, Dutta R, Žiarovská J, Tzvetkov NT, Severová L, Kopecká L, Milella L, Fernández-Cusimamani E. Repurposing Major Metabolites of Lamiaceae Family as Potential Inhibitors of α-Synuclein Aggregation to Alleviate Neurodegenerative Diseases: An in Silico Approach. Front Pharmacol. 2025;16:1519145. https://doi.org/10.3389/fphar.2025.1519145
59. Kondratyev M, Rudnev V, Nikolsky K, Petrovsky D, Kulikova L, Malsagova K, Stepanov A, Kopylov A, Kaysheva A. In Silico Study of the Interactions of Anle138b Isomer, an Inhibitor of

Amyloid Aggregation with Partner Proteins. Int J Mol Sci. 2022;23(24):16096. https://doi.org/10.3390/ijms232416096

60. Semenyuk P. REMD Simulations of Full-Length Alpha-Synuclein together with Ligands Reveal Binding Region and Effect on Amyloid Conversion. Int J Mol Sci. 2022;23(19):11545. https://doi.org/10.3390/ijms231911545
61. Killinger B, Melki R, Brundin P, Kordower J. Endogenous Alpha-Synuclein Monomers, Oligomers and Resulting Pathology: Let's Talk About the Lipids in the Room. NPJ Parkinsons Dis. 2019;5:23. https://doi.org/10.1038/s41531-019-0095-3
62. Tira R, De Cecco E, Rigamonti V, Santambrogio C, Barracchia C, Munari F, Romeo A, Legname G, Prosperi D, Grandori R, Assfalg M. Dynamic Molecular Exchange and Conformational Transitions of Alpha-Synuclein at the Nano-Bio Interface. Int J Biol Macromol. 2020;165(Pt A):562–571. https://doi.org/10.1016/j.ijbiomac.2020.03.118
63. Bhullar K, Rupasinghe H. Polyphenols: Multipotent Therapeutic Agents in Neurodegenerative Diseases. Oxid Med Cell Longev. 2013;2013:891748. https://doi.org/10.1155/2013/891748
64. de Lima E, Laurindo L, Catharin V, Direito R, Tanaka M, German I, Lamas C, Guiguer E, Araújo A, Fiorini A, Barbalho S. Polyphenols, Alkaloids, and Terpenoids against Neurodegeneration: Evaluating the Neuroprotective Effects of Phytocompounds through a Comprehensive Review of the Current Evidence. Metabolites. 2025;15(2):124. https://doi.org/10.3390/metabo15020124
65. Henríquez G, Gomez A, Guerrero E, Narayan M. The Potential Role of Natural Polyphenols against Protein Aggregation Toxicity: In Vitro, In Vivo and Clinical Studies. ACS Chem Neurosci. 2020;11(19):2919–2934. https://doi.org/10.1021/acschemneuro.0c00381
66. Rocha E, De Miranda B, Sanders L. Alpha-Synuclein: Pathology, Mitochondrial Dysfunction and Neuroinflammation in Parkinson's Disease. Neurobiol Dis. 2018;109(Pt B):249–257. https://doi.org/10.1016/j.nbd.2017.04.004
67. Sohrabi T, Mirzaei-Behbahani B, Zadali R, Pirhaghi M, Morozova-Roche L, Meratan A. Common Mechanisms Underlying α-Synuclein-Induced Mitochondrial Dysfunction in Parkinson's Disease. J Mol Biol. 2023;435(12):167992. https://doi.org/10.1016/j.jmb.2023.167992
68. Yedlapudi D, Joshi G, Luo D, Todi S, Dutta A. Inhibition of Alpha-Synuclein Aggregation by Multifunctional Dopamine Agonists Assessed by a Novel in Vitro Assay and an in Vivo Drosophila Synucleinopathy Model. Sci Rep. 2016;6:38510. https://doi.org/10.1038/srep38510
69. Yedlapudi D, Xu L, Luo D, Marsh G, Todi S, Dutta A. Targeting Alpha Synuclein and Amyloid Beta by a Multifunctional, Brain-Penetrant Dopamine D2/D3 Agonist D-520: Potential

Therapeutic Application in Parkinson's Disease with Dementia. Sci Rep. 2019;9(1):19744. https://doi.org/10.1038/s41598-019-55830-3

70. Dinda B, Das B, Biswas S, Sharma H, Armstrong C, Yedlapudi D, Antonio T, Reith M, Dutta A. Bivalent Dopamine Agonists with Co-Operative Binding and Functional Activities at Dopamine D2 Receptors, Modulate Aggregation and Toxicity of Alpha Synuclein Protein. Bioorg Med Chem. 2022;78:117131. https://doi.org/10.1016/j.bmc.2022.117131
71. Luo D, Sharma H, Yedlapudi D, Antonio T, Reith M, Dutta A. Novel Multifunctional Dopamine D2/D3 Receptors Agonists with Potential Neuroprotection and Anti-Alpha Synuclein Protein Aggregation Properties. Bioorg Med Chem. 2016;24(21):5088–5102. https://doi.org/10.1016/j.bmc.2016.08.021
72. Omoboyowa D, Balogun T, Omomule O, Saibu O. Identification of Terpenoids from Abrus Precatorius Against Parkinson's Disease Proteins Using In Silico Approach. Bioinform Biol Insights. 2021;15:11779322211050757. https://doi.org/10.1177/11779322211050757
73. Ono K, Tsuji M, Yamasaki T, Pasinetti G. Anti-Aggregation Effects of Phenolic Compounds on α-Synuclein. Molecules. 2020;25(10):2444. https://doi.org/10.3390/molecules25102444
74. Yu L, Li X, Shi T, Li N, Zhang D, Liu X, Xiao Y, Liu X, Petersen RB, Xue W, Yu YV, Hu DS, Xu L, Chen H, Zheng L, Huang K, Peng A. Identification of Novel Phenolic Inhibitors from Traditional Chinese Medicine against Toxic α-Synuclein Aggregation via Regulating Phase Separation. Int J Biol Macromol. 2025;297:139875. https://doi.org/10.1016/j.ijbiomac.2025.139875
75. Chakroun T, Evsyukov V, Nykänen NP, Höllerhage M, Schmidt A, Kamp F, Ruf VC, Wurst W, Rösler TW, Höglinger GU. Alpha-Synuclein Fragments Trigger Distinct Aggregation Pathways. Cell Death Dis. 2020;11(2):84. https://doi.org/10.1038/s41419-020-2285-7
76. Vidović M, Rikalovic M. Alpha-Synuclein Aggregation Pathway in Parkinson's Disease: Current Status and Novel Therapeutic Approaches. Cells. 2022;11(11):1732. https://doi.org/10.3390/cells11111732

| *Received: 22 julio 2026]* | *Accepted: [1 septiembre 2026]* | *Published: [15 noviembre 2026]* |

Citation: *Quiroz,* Y; *Delgado, A; Mora, M; Vivas, A; Bravo*, Y; *Alvarado, Y; González-Paz, L* Interaction Mechanisms of Bioactive Compounds with α-Synuclein: A Docking and Molecular Dynamics Study. *Bionatura*. 2026. Volumen 11, No 3

Peer review information: Bionatura thanks the anonymous reviewers for their contribution to the peer review of this work using https://reviewerlocator.webofscience.com/

ISSN 1390-9355
Vol.11. No 3. 2026

All articles published by Bionatura Journal are freely and permanently accessible online immediately after publication, without subscription charges or registration barriers.

Publisher's Note: Bionatura stays neutral concerning jurisdictional claims in published maps and institutional affiliations.

Copyright: © 2026 by the authors. Submitted for possible open access publication under the terms and conditions of the Creative Commons Attribution (CC BY) license (https://creativecommons.org/licenses/by/4.0/)